



## Racemic peptide assembly boosts biocatalysis†

Cite this: *Org. Biomol. Chem.*, 2025, **23**, 2797

Mari C. Mañas-Torres,<sup>a,b</sup> Paola Alletto,<sup>a</sup> Simone Adorinni,<sup>a</sup> <sup>a</sup> Attilio V. Vargiu,<sup>c</sup> Luis Álvarez de Cienfuegos<sup>b</sup> and Silvia Marchesan \*<sup>a</sup>

Received 8th December 2024,

Accepted 11th February 2025

DOI: 10.1039/d4ob01987c

rsc.li/obc

**Racemic assembly of minimalistic heterochiral tripeptides boosts their biocatalytic activity for ester hydrolysis. The amino acidic sequences are bioinspired and feature histidine (His) as a catalytically active residue, and the diphenylalanine (Phe-Phe) motif to drive self-assembly into anisotropic nanostructures that gel. This study thus provides key insights for the design of green biocatalysts with improved activity.**

The pressure that our society is facing to implement the transition towards greener processes is well-known. In particular, biocatalysis,<sup>1</sup> together with organocatalysis<sup>2</sup> and photocatalysis,<sup>3</sup> is an attractive approach to make chemical transformations greener and more efficient. To this end, enzymes have been largely used and, in particular, hydrolases have entered a wide variety of industrial processes and even many consumer products.<sup>4</sup> However, not many of them come at the low cost and with the robustness required for industrial use on a large scale. It is thus not surprising that minimalistic approaches that use short peptides for their mimicry have gathered momentum. These building blocks are economical and easy to make, and they withstand a large variety of physico-chemical conditions.<sup>5</sup> Furthermore, a key advantage is the possibility to encode the biocatalytic activity in their supramolecular assemblies that create hydrophobic pockets similarly to enzymes.<sup>6–8</sup> In this manner, smart catalysts can be switched on/off with assembly/disassembly, thus opening the way to exciting avenues, such as the mimicry of biochemical pathways<sup>9</sup> or the ad-hoc control over products' formation, for instance for the design of out-of-equilibrium systems<sup>10</sup> or to trigger reaction cascades for targeted therapy.<sup>11</sup>

In particular, the amino acid histidine (His) plays a key role in a large variety of enzymatic catalytic sites, and it is widely studied as a building block for functional assemblies.<sup>12</sup> Furthermore, His plays crucial roles in interfacing biomolecules with inorganic components towards the generation of complex bioinspired functional structures, thus its derivatives could find further applications that go well beyond catalysis.<sup>13</sup> A few examples have been reported of ultrashort peptides bearing His that are capable of hydrolase mimicry when self-assembled at neutral pH, such as cyclo (His-Phe),<sup>14</sup> Fmoc-Phe-Phe-His-NH<sub>2</sub> and Fmoc-Phe-Phe-Arg-NH<sub>2</sub>,<sup>15</sup> and ferrocenyl-Phe-Phe-His.<sup>16</sup> The introduction of D-amino acids can confer further advantages, such as increased resistance against enzymatic degradation. For this reason, we designed L-His-D-Phe-D-Phe that is catalytic only in its assembled state.<sup>17</sup> Subsequent studies demonstrated that C-terminal amidation enables a five-fold improvement in catalytic activity under analogous conditions.<sup>18</sup> Conversely, other modifications, such as N-acetylation or peptide elongation to include Ser to serve as nucleophile, resulted in detrimental effects in catalytic performance and/or gelation ability, thus demonstrating that the design of such minimalistic supramolecular catalysts is not trivial.<sup>18,19</sup>

In light of these results, we selected the best-performing catalytic gelator identified from our previous research endeavours, *i.e.* L-His-D-Phe-D-Phe-NH<sub>2</sub> (Hff), and studied its equimolar co-assembly with its enantiomer, D-His-L-Phe-L-Phe-NH<sub>2</sub> (hFF) (Fig. 1A), as a different strategy to further improve catalytic activity. We took inspiration from studies led by Schneider that reported racemic peptide assemblies with synergistic assembling behaviour leading to more rigid hydrogels, relative to each enantiomer alone.<sup>20</sup> Subsequently, the same group demonstrated the molecular basis for such an effect, revealing that the two enantiomers were alternating in the co-assembled rippled β-sheet,<sup>21</sup> which is a structure that was predicted by Pauling and Corey in 1953.<sup>22</sup> The racemic co-assembly is held together by hydrogen bonds within the sheet, thus, creating nested hydrophobic interactions between enantiomers in the dry fibrils' interior that do not occur in the case

<sup>a</sup>Chem. Pharm. Sc. Dept., University of Trieste, Via L. Giorgieri 1, Trieste 34127, Italy. E-mail: smarchesan@units.it

<sup>b</sup>Departamento de Química Orgánica, Facultad de Ciencias, Universidad de Granada (UGR), 18071 Granada, Spain

<sup>c</sup>Department of Physics, University of Cagliari, Cittadella Universitaria, S.P. 8 km. 0.7, 09042 Monserrato, CA, Italy

† Electronic supplementary information (ESI) available: Spectroscopic and microscopic data. See DOI: <https://doi.org/10.1039/d4ob01987c>



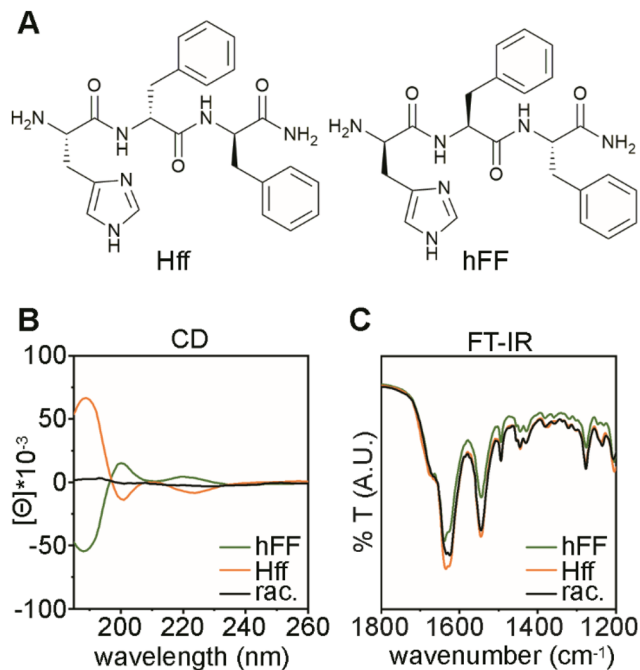


**Fig. 1** (A) Chemical structures of the two enantiomers Hff (left) and hFF (right). (B) Circular dichroism (CD) spectra of Hff, hFF, and their racemic mixture at 1 mM. (C) FT-IR spectra of the amide region of Hff, hFF, and their racemic mixture.

of enantiopure assemblies. We reasoned that the maximization of such hydrophobic regions could enhance hydrophobic substrate binding for catalysis.

The two enantiomers were synthesised, purified by HPLC, freeze-dried, and their identity and purity were confirmed by  $^1\text{H}$ - and  $^{13}\text{C}$ -NMR, and ESI-MS spectra (ESI, S1–S4 $^\dagger$ ). Their circular dichroism (CD) spectra (Fig. 1B) were mirror-imaged, while their equimolar mixture was featureless, as expected. The CD signatures were reminiscent of those of other heterochiral tripeptides forming amphipathic  $\beta$ -sheets upon assembly, and characterised by two main peaks at 200 and 220 nm. $^{23}$  Upon assembly conditions at higher concentrations, the CD spectra could be acquired only above 215 nm due to scattering, and maintained the same features (ESI, Section S5 $^\dagger$ ). Fourier-transformed infrared spectra (FT-IR, Fig. 1C) revealed the typical signals of  $\beta$ -sheets in the amide I and II regions, at 1632 and 1542  $\text{cm}^{-1}$ , respectively. Microscopy analyses were also performed. Atomic force microscopy (AFM) and scanning electron microscopy (SEM) images revealed anisotropic structures. No significant difference was found in the fibers' width across samples (Fig. 2, bottom), corresponding to a median of  $105 \pm 18$  nm for hFF,  $104 \pm 17$  nm for Hff, and  $107 \pm 18$  nm for the racemic mixture ( $n = 100$  counts).

Oscillatory rheology was then used to assess the viscoelastic properties of the hydrogels (Fig. 3). The two enantiomers displayed similar behaviour. Time sweeps revealed immediate gelation and an increasing elastic modulus ( $G'$ ) over one hour until  $34.3 \pm 5.0$  kPa for hFF, and  $34.9 \pm 3.4$  kPa for Hff. By con-

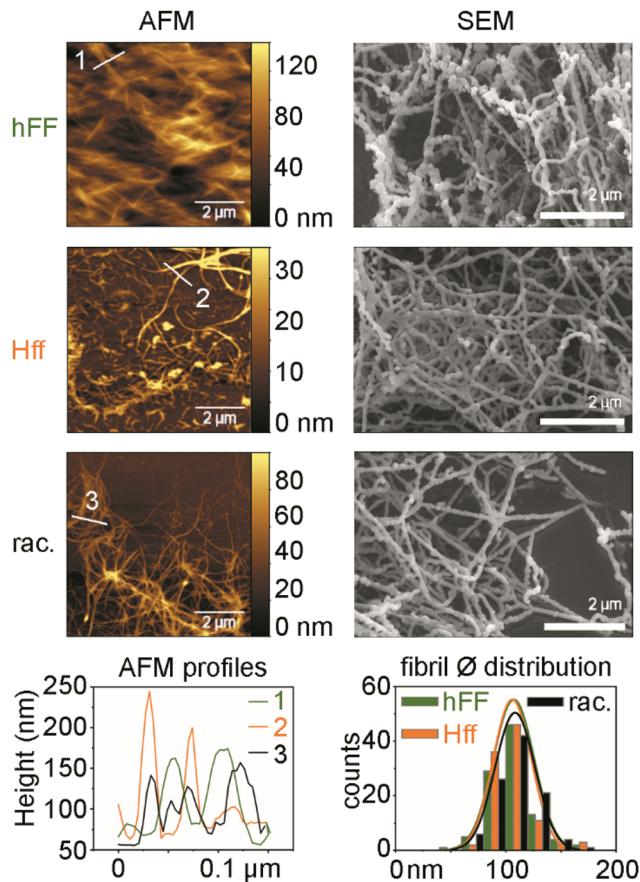


**Fig. 2** AFM (left) and SEM (right) images of the peptide fibers and their width determined by AFM profiles (bottom left) and size distribution from SEM analyses (bottom right).

trast, the racemic mixture displayed a 15 min lag time, with  $G'$  reaching a plateau after  $\sim 3$  h. Remarkably,  $G'$  of the racemic mixture reached  $592 \pm 45$  kPa, corresponding to a  $\sim 17$ -fold increase relative to each enantiomer alone. Furthermore, stress sweeps demonstrated that the racemic gel displayed also enhanced resistance against applied stress, with gel-to-sol transition occurring above 300 Pa, in contrast with each enantiomer whose moduli dropped at 70 Pa. Overall, the enhancement in the viscoelastic properties was consistent with the expected behaviour for the co-assembled rippled  $\beta$ -sheet. $^{17}$  Single-crystal X-ray diffraction is the technique of choice to confirm the enantiomeric peptide alternation in the stacks, $^{24}$  but unfortunately all our attempts to crystallize Hff, hFF, or their racemic mixture were unsuccessful.

Finally, we tested the assemblies for catalytic hydrolysis of *p*-nitrophenyl acetate (pNPA) as a chromogenic substrate (Fig. 4A). $^{25}$  The parent compound Hff-COOH was reported to display a  $k_{\text{obs}} = 3.5 \times 10^{-4} \text{ s}^{-1}$  when tested in the form of fibrils (25 mM) with 0.2 mM pNPA. $^{17}$  C-terminally amidated Hff performed similarly, also at two-fold concentration to yield a hydrogel (*i.e.*,  $k_{\text{obs}} = 3.6 \times 10^{-4} \text{ s}^{-1}$ ). $^{18}$  In this work, when tested with 1 mM pNPA, both Hff and hFF fibrils (25 mM) displayed a  $k_{\text{obs}} = 4.5 \times 10^{-4} \text{ s}^{-1}$ . Remarkably, the racemic mixture with



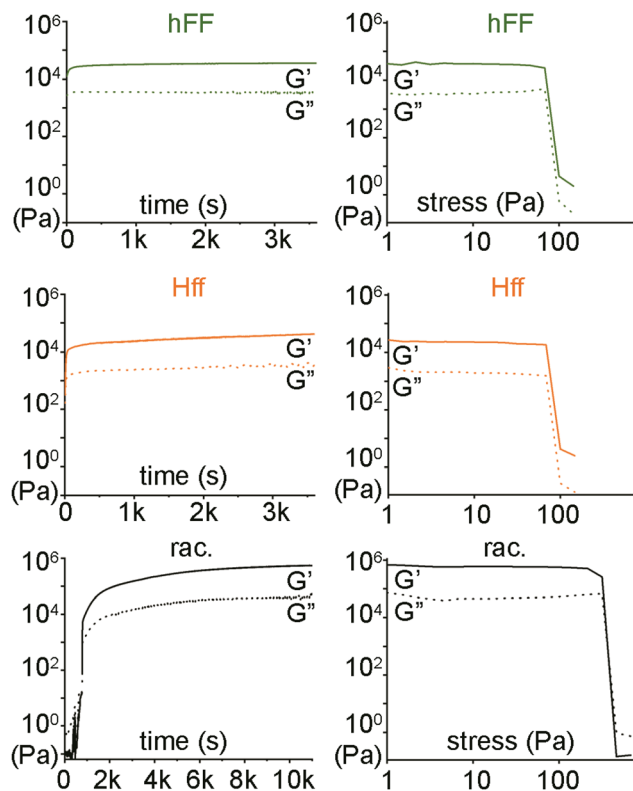


**Fig. 3** Oscillatory rheology analysis of the hydrogels formed by each enantiomer (hFF, green, top and Hff, orange, middle) and by their racemic mixture (rac., black, bottom). Time sweeps are shown on the left, and stress sweeps on the right.

the same peptide total concentration (*i.e.* = 25 mM obtained from 12.5 mM of each enantiomer) showed a further improvement by over 50% corresponding to a  $k_{\text{obs}} = 7.0 \times 10^{-4} \text{ s}^{-1}$ . To the best of our knowledge, this is the first report of a self-assembled catalyst whereby the racemic mixture displays improved catalysis relative to each enantiomer alone, which suggests the presence of organized co-assembled peptide fibrils, in agreement with spectroscopic and microscopic data that are compatible with the presence of rippled  $\beta$ -sheets. The presence of more hydrophobic pockets in the co-assembled catalyst that could favor substrate binding, and lead to enhanced catalysis, was then verified by fluorescence measurements using 8-anilino-naphthalene-1-sulfonate ammonium salt (ANS). The use of this fluorophore is well-established to monitor the formation of hydrophobic environments, such as those arising upon peptide self-assembly.<sup>26,27</sup> In particular, ANS fluorescence undergoes a blue-shift and increase in intensity when it is located in more hydrophobic environments,<sup>28</sup> and this was also our case, as shown in Fig. 4D. ANS alone displayed a mild fluorescence with a broad peak centred at 475 nm in the 450–500 nm range. A blueshift to 455 nm occurred when ANS was embedded in peptide assemblies, and fluorescence intensity increased 2-fold and 3-fold, in case of enantiopure and racemic assemblies, respectively. We inferred the presence of more hydrophobic pockets in the latter, as

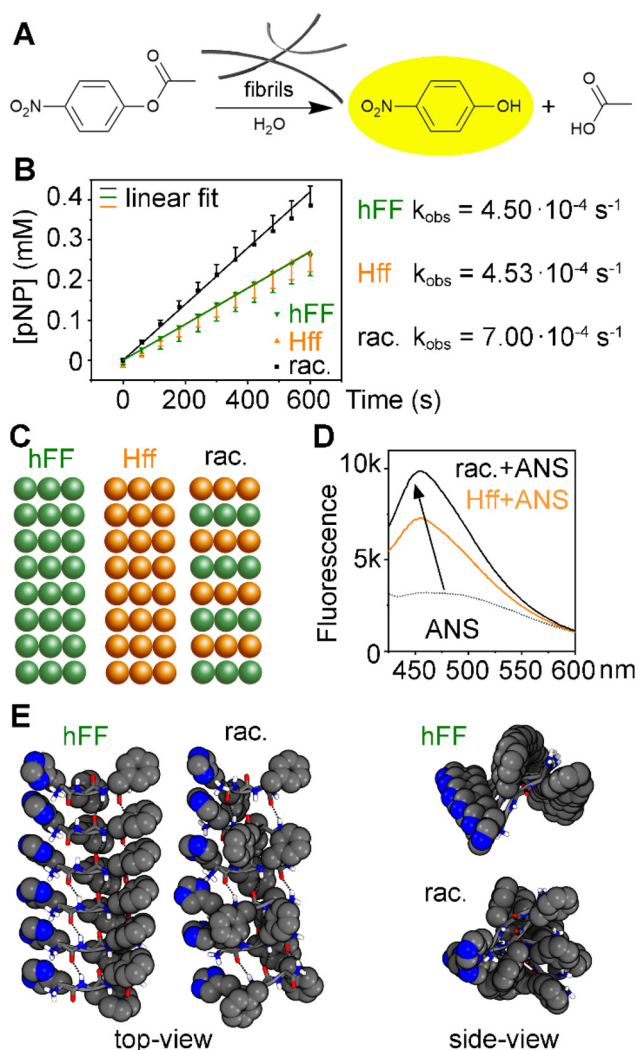


**Fig. 4** (A) Reaction scheme for *p*-nitrophenyl acetate (pNPA) hydrolysis catalysed by peptide fibrils to yield yellow *p*-nitrophenol (pNP). (B) Initial reaction rate in the presence of fibrils of hFF, Hff, or their racemic mixture (rac.). (C) Scheme of the proposed assemblies of enantiopure stacks for hFF or Hff, and of alternating enantiomers for the racemic mixture. (D) Fluorescence emission of ANS in Hff and racemic (rac.) peptide fibers, and in solution. (E) Molecular models of the sheets formed by hFF and rac. reveal the presence of evident hydrophobic pockets for the latter.

expected for rippled  $\beta$ -sheets. This hypothesis was confirmed by minimalistic molecular models (Fig. 4E), which revealed a hydrophobic crevice lined by the Phe rings only in the racemic assembly.

In conclusion, this proof of concept work describes the spectroscopic, microscopic, and rheological behaviour of a racemic mixture composed of a minimalistic tripeptide sequence that bears His for hydrolase mimicry,<sup>6,29,30</sup> and Phe-Phe<sup>31,32</sup> as a self-assembling motif. All the data support the formation of a rippled  $\beta$ -sheet, which was already described as a useful type of assembly for racemic tripeptides,<sup>24</sup> as well as longer peptides to yield supramolecular hydrogels with



increased stiffness.<sup>16</sup> Importantly, this is the first work that proposes the use of racemic minimalistic tripeptide co-assemblies for enhanced biocatalysis, thus opening the way to the use of this approach to develop green catalysts. Given that peptide catalysts' optimization based on expert-knowledge-guided discovery is not trivial, we anticipate that integration with machine-learning approaches will be key to speed up advances in the field.<sup>33,34</sup> The vast progress in peptide modelling methods,<sup>35</sup> with the concomitant generation of curated datasets for catalytic peptides<sup>36</sup> are important steps ahead to enable rapid developments. Indeed, combination of *in silico* and experimental approaches is already being successful to shed new light on the structure–activity relationship of catalytic amyloids,<sup>37</sup> and looks promising to unveil key mechanistic details to unlock their full potential in various applications.

## Data availability

The data supporting this article have been included as part of the ESI.†

## Conflicts of interest

There are no conflicts to declare.

## Acknowledgements

This work was supported by funding from the Italian Ministry of University and Research (MUR) through the PRIN program, grant no. 2022XEZK7K (SHAZAM) to S. M. funded by the European Union – Next Generation EU. M. C. M. T. acknowledges grant PRE2018-083773 funded by MCIN/AEI/10.13039/501100011033 and FSE “El FSE invierte en tu futuro”, Spain. L. A. C. acknowledges grant PID2023-150318NB-I00 funded by MCIU/AEI/10.13039/501100011033, Spain. This article is based upon work from COST Action CA23111 SNOOPY, supported by COST (European Cooperation in Science and Technology).

## References

- 1 R. Buller, S. Lutz, R. J. Kazlauskas, R. Snajdrova, J. C. Moore and U. T. Bornscheuer, *Science*, 2023, **382**, eadh8615.
- 2 C. Rizzo, A. Pace, I. Pibiri, S. Buscemi and A. Palumbo Piccionello, *ChemSusChem*, 2024, **17**, e202301604.
- 3 G. Goti, K. Manal, J. Sivaguru and L. Dell'Amico, *Nat. Chem.*, 2024, **16**, 684–692.
- 4 E. R. Tatta, M. Imchen, J. Moopantakath and R. Kumavath, *Appl. Microbiol. Biotechnol.*, 2022, **106**, 1813–1835.
- 5 P. Alletto, A. M. Garcia and S. Marchesan, *Gels*, 2023, **9**, 678.
- 6 P. Janković, M. Babić, M. Perčić, A. S. Pina and D. Kalafatovic, *Mol. Syst. Des. Eng.*, 2023, **8**, 1371–1380.
- 7 Q. Liu, A. Kuzuya and Z.-G. Wang, *iScience*, 2023, **26**, 105831.
- 8 Y. Lou, B. Zhang, X. Ye and Z.-G. Wang, *Mater. Today Nano*, 2023, **21**, 100302.
- 9 M. D. Pol, R. Thomann, Y. Thomann and C. G. Pappas, *J. Am. Chem. Soc.*, 2024, **146**, 29621–29629.
- 10 G. Olivo, G. Capocasa, D. Del Giudice, O. Lanzalunga and S. Di Stefano, *Chem. Soc. Rev.*, 2021, **50**, 7681–7724.
- 11 H. Wang, D. Jiao, D. Feng, Q. Liu, Y. Huang, J. Hou, D. Ding and W. Zhang, *Adv. Mater.*, 2024, **36**, 2311733.
- 12 O. S. Tiwari, R. Aizen, M. Meli, G. Colombo, L. J. W. Shimon, N. Tal and E. Gazit, *ACS Nano*, 2023, **17**, 3506–3517.
- 13 Y. Chen, K. Tao, W. Ji, V. B. Kumar, S. Rencus-Lazar and E. Gazit, *Mater. Today*, 2022, **60**, 106–127.
- 14 A. J. Kleinsmann and B. J. Nachtsheim, *Org. Biomol. Chem.*, 2020, **18**, 102–107.
- 15 Z. Huang, S. Guan, Y. Wang, G. Shi, L. Cao, Y. Gao, Z. Dong, J. Xu, Q. Luo and J. Liu, *J. Mater. Chem. B*, 2013, **1**, 2297–2304.
- 16 X. Yang, Y. Wang, W. Qi, R. Su and Z. He, *Nanoscale*, 2017, **9**, 15323–15331.
- 17 A. M. Garcia, M. Kurbasic, S. Kralj, M. Melchionna and S. Marchesan, *Chem. Commun.*, 2017, **53**, 8110–8113.
- 18 M. Kurbasic, A. M. Garcia, S. Viada and S. Marchesan, *Molecules*, 2021, **26**, 173.
- 19 M. Kurbasic, A. M. Garcia, S. Viada and S. Marchesan, *J. Pept. Sci.*, 2022, **28**, e3304.
- 20 K. J. Nagy, M. C. Giano, A. Jin, D. J. Pochan and J. P. Schneider, *J. Am. Chem. Soc.*, 2011, **133**, 14975–14977.
- 21 K. Nagy-Smith, P. J. Beltramo, E. Moore, R. Tycko, E. M. Furst and J. P. Schneider, *ACS Cent. Sci.*, 2017, **3**, 586–597.
- 22 L. Pauling and R. B. Corey, *Proc. Natl. Acad. Sci. U. S. A.*, 1953, **39**, 253–256.
- 23 A. M. Garcia, D. Iglesias, E. Parisi, K. E. Styan, L. J. Waddington, C. Deganutti, R. De Zorzi, M. Grassi, M. Melchionna, A. V. Vargiu and S. Marchesan, *Chem*, 2018, **4**, 1862–1876.
- 24 A. Hazari, M. R. Sawaya, N. Vlahakis, T. C. Johnstone, D. Boyer, J. Rodriguez, D. Eisenberg and J. A. Raskatov, *Chem. Sci.*, 2022, **13**, 8947–8952.
- 25 P. Janković and D. Kalafatovic, *Methods Enzymol.*, 2024, **697**, 423–433.
- 26 C. J. C. Edwards-Gayle, V. Castelletto, I. W. Hamley, G. Barrett, F. Greco, D. Hermida-Merino, R. P. Rambo, J. Seitsonen and J. Ruokolainen, *ACS Appl. Bio Mater.*, 2019, **2**, 2208–2218.
- 27 N. Balasco, D. Altamura, P. L. Scognamiglio, T. Sibillano, C. Giannini, G. Morelli, L. Vitagliano, A. Accardo and C. Diaferia, *Langmuir*, 2024, **40**, 1470–1486.
- 28 N. Singh, M. P. Conte, R. V. Ulijn, J. F. Miravet and B. Escuder, *Chem. Commun.*, 2015, **51**, 13213–13216.
- 29 M. Bélières, N. Chouini-Lalanne and C. Déjugnat, *RSC Adv.*, 2015, **5**, 35830–35842.



- 30 C. M. Rufo, Y. S. Moroz, O. V. Moroz, J. Stöhr, T. A. Smith, X. Hu, W. F. DeGrado and I. V. Korendovych, *Nat. Chem.*, 2014, **6**, 303–309.
- 31 M. Reches and E. Gazit, *Science*, 2003, **300**, 625–627.
- 32 E. Mayans and C. Alemán, *Molecules*, 2020, **25**, 6037.
- 33 T. Schnitzer, M. Schnurr, A. F. Zahrt, N. Sakhaee, S. E. Denmark and H. Wennemers, *ACS Cent. Sci.*, 2024, **10**, 367–373.
- 34 M. Ramakrishnan, A. van Teijlingen, T. Tuttle and R. V. Ulijn, *Angew. Chem., Int. Ed.*, 2023, **62**, e202218067.
- 35 A. van Teijlingen, D. C. Edwards, L. Hu, A. Lilienkampf, S. L. Cockroft and T. Tuttle, *Phys. Chem. Chem. Phys.*, 2024, **26**, 17745–17752.
- 36 P. Janković, E. Otović, G. Mauša and D. Kalafatovic, *Data Brief*, 2023, **48**, 109290.
- 37 L. Roldan, L. Rodríguez-Santiago, J. Didier-Marechal and M. Sodupe, *Chem. – Eur. J.*, 2024, **30**, e202401797.

